

FULL PAPER

Ferromagnetic nanoparticle-supported copper complex: A highly efficient and reusable catalyst for three-component syntheses of 1,4-disubstituted 1,2,3-triazoles and C–S coupling of aryl halides

Mohammad Mehdi Khodaei | Kiumars Bahrami | Farhat Sadat Meibodi

Department of Organic Chemistry, Faculty of Chemistry, Razi University, Kermanshah 67149-67346, Iran

Correspondence

Mohammad Mehdi Khodaei and Kiumars Bahrami, Department of Organic Chemistry, Faculty of Chemistry, Razi University, Kermanshah 67149-67346, Iran.
Email: mmkhoda@razi.ac.ir;
kbahrami2@hotmail.com

A new nanocatalyst was synthesized by immobilization of 4'-(4-hydroxyphenyl)-2,2':6',2''-terpyridine/CuI complex on ferromagnetic nanoparticles through a surface modification (FMNPs@SiO₂-TPy-Cu). This heterogeneous catalyst was characterized using various techniques including Fourier transform infrared and energy-dispersive X-ray spectroscopies, transmission and scanning electron microscopies, X-ray diffraction, vibrating sample magnetometry and thermogravimetric analysis. The resulting nanocatalyst presented excellent catalytic activity for the regioselective syntheses of 1,4-disubstituted 1,2,3-triazoles and thioethers. The thermally and chemically stable, benign and economical catalyst was easily recovered using an external magnet and reused in at least five successive runs without an appreciable loss of activity.

KEYWORDS

1,2,3-triazole, C–S coupling reaction, immobilized copper catalyst, magnetic nanoparticles, terpyridines

1 | INTRODUCTION

The most important industrial disadvantages of performing homogeneously catalysed reactions are the difficulties of separating the catalyst from the product and reusing the expensive catalyst. These problems could be solved by heterogenation of existing homogeneous catalysts. Thus, many attempts have been made to develop heterogenation of catalysts using various types of support such as polymeric, organic and inorganic supports.^[1] Even though heterogeneous catalytic systems can be recovered and reused, the active sites in heterogeneous catalysts are not as accessible as in homogeneous catalysts, so the activity of the catalysts are usually decreased. As a result, we need a catalyst system to have high activity and selectivity in addition to being easy to separate and recover. Nanocatalysts can bridge the gap between homogeneous and heterogeneous systems, keeping the desirable attributes of both systems.^[2] With the advent of nanotechnology in the manufacture of catalysts, nanocatalysts can be produced with high economic efficiency, high safety and optimal use of chemicals and raw

materials.^[3] Despite these advantages for heterogeneous catalysts, expensive ultracentrifugation is often the only way to separate product and catalyst.^[4] Magnetization of catalysts can solve this problem since they can be easily separated from the reaction mixture using an external permanent magnet.^[5]

Huisgen cycloaddition reactions of organic azides with alkynes are promoted by copper catalysts with excellent efficiency and selectivity.^[6] This reaction has found many applications in various research areas including bioorganic chemistry, medicinal chemistry and material science.^[7] For example, the 1,2,3-triazole core is a key structural motif in many bioactive compounds, exhibiting a wide range of activities, such as anti-inflammatory, anti-tubercular, anticancer, antibacterial, antimicrobial, anti-allergic and anticonvulsant activities.^[8] The reaction proceeds with high regioselectivity when using terminal alkynes and produces 1,4-disubstituted 1,2,3-triazines as sole product.^[9] The use of Cu(I)^[10] and Cu(II)/reducing agent (often sodium ascorbate or metallic copper)^[11] and metallic copper^[12] has been reported in many articles. However, due to the advantages of heterogeneous

catalysts, such as recovery and reusability, various supported copper catalysts have been applied.^[13] Although there are many reports on this topic, there is still a need to develop methods for the synthesis of 1,4-disubstituted 1,2,3-triazoles which has received less attention.

The C–S bond formation of aryl halides with thiols is a valuable step in the synthesis of many compounds that are of biological, pharmaceutical and materials interest.^[14] For example, sulfide is a common functionality found in many drugs in use for the treatment of diabetes, inflammation and Parkinson's and Alzheimer's diseases.^[15] Transition metal-catalysed cross-coupling reactions between aryl halides and thiols suggest a strong strategy for the construction of C–S bonds. Despite the importance of this reaction protocol in organic synthesis, less attention has been paid to transition metal-catalysed thioetherification, compared to other carbon–heteroatom bond forming reactions.

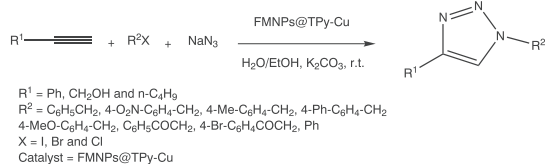
The first report of C–S coupling reaction was by Migita and co-workers^[16] in which they used Pd(PPh₃)₄ as a catalyst for the reaction of aryl iodides and bromides with thiols. Many other palladium-based catalyst systems with bidentate phosphines or diverse organophosphate derivatives have also been reported^[17] but these systems have disadvantages such as the use of the prepared PR₃ ligands which are not eco-friendly. Other transition metal catalysts based on nickel^[18] and cobalt^[19] have also been investigated for the formation of C–S bonds. These catalysts have certain disadvantages such as metal toxicity. Consequently, further development of copper-based catalytic systems is still required because of the low cost of copper, despite many reports using copper as catalyst.^[20]

In continuation of our previous efforts to develop new organic–inorganic hybrid materials as heterogeneous catalysts,^[21] a new reusable and efficient heterogeneous ferromagnetic nanoparticle-supported copper(I) iodide (FMNPs@TPy-Cu) catalyst is introduced for the synthesis of 1,4-disubstituted 1,2,3-triazoles from organic halides, sodium azide and terminal alkynes in water and ethanol at room temperature (Scheme 1) and for C–S bond formation in cross-coupling reactions of aryl halides and thiols in dimethylformamide (DMF) (Scheme 2).

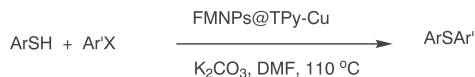
2 | EXPERIMENTAL

2.1 | Materials and physical measurements

The materials were purchased from Merck and Fluka and were used without any additional purification. All reactions



SCHEME 1 Preparation of 1,4-disubstituted 1,2,3-triazoles in the presence of FMNPs@TPy-Cu as nanocatalyst



$\text{Ar} = 4\text{-Me-C}_6\text{H}_4, 4\text{-O}_2\text{N-C}_6\text{H}_4, \text{Ph}$
 $\text{Ar}' = \text{C}_6\text{H}_5, 4\text{-Me-C}_6\text{H}_4, 2\text{-Me-C}_6\text{H}_4, 4\text{-MeO-C}_6\text{H}_4, 4\text{-O}_2\text{N-C}_6\text{H}_4, 4\text{-Br-C}_6\text{H}_4, \text{C}_4\text{H}_9\text{S}$
 $\text{X} = \text{I, Br}$
 Catalyst = FMNPs@TPy-Cu

SCHEME 2 Preparation of thioethers through carbon (aryl)–sulfur coupling reaction in the presence of FMNPs@TPy-Cu as nanocatalyst

were monitored by TLC. Melting points were determined using a Stuart Scientific SMP2 apparatus. Fourier transform infrared (FT-IR) spectra were obtained with a Perkin Elmer 683 instrument. ¹H NMR and ¹³C NMR spectra were recorded with a Bruker (300 MHz) spectrometer using CDCl₃ as solvent. Powder X-ray diffraction (XRD) patterns were obtained with a SEIFERT-3003TT. Scans were taken with a 2θ step size of 0.02° from 3° to 70° and a counting time of 1.0 s using a Cu K_α radiation source (λ = 1.542 Å) and a nickel filter. Thermogravimetric analysis (TGA) was carried out with a PL-STA-1640 in the range 30–600 °C with a heating rate of 10 °C min^{−1}. Scanning electron microscopy (SEM) was performed with a VEGA 20 TESCAN microscope. Transmission electron microscopy (TEM) measurements were carried out with a Zeiss-EM10C (Germany) operating at 80 kV and using formvar carbon-coated grid Cu mesh 300. Energy-dispersive X-ray (EDX) spectroscopy patterns were measured using a Seron model AIS2300C. Magnetic measurements were carried out using vibrating sample magnetometry (VSM; BHV-55 and Riken, Japan) at room temperature. All of the known products were characterized by comparison of their spectral data and physical properties with those reported in the literature.

2.2 | Preparation of catalyst

2.2.1 | Preparation of ferromagnetic nanoparticles (FMNPs)

FMNPs modified with citrate groups were prepared according to a reported procedure.^[22] Iron(III) chloride hexahydrate (5.40 g, 20 mmol) and iron(II) chloride tetrahydrate (2 g, 10 mmol) were dissolved in deionized water (120 ml) under nitrogen atmosphere. Then, 10 ml of ammonium hydroxide (25%) was quickly added into the solution under rapid mechanical stirring (500 rpm) and the mixture was heated to 60 °C, while being stirred vigorously with a mechanical stirrer for 1 h under nitrogen atmosphere. After cooling to room temperature, the resultant nanoparticles were gathered using a magnet and the collected magnetic solid was dispersed in 200 ml of trisodium citrate solution (0.3 M) and heated at 80 °C for 1 h. Finally, the precipitates were collected using an external magnet and washed with acetone to eliminate remaining trisodium citrate.

2.2.2 | Preparation of silica-coated FMNPs (FMNPs@SiO₂)

The surface-modified FMNPs (1 g) were dispersed in deionized water (40 ml) and ethanol by the ultrasonic treatment for

25 min. Then $\text{NH}_3\cdot\text{H}_2\text{O}$ (5 ml) and a solution of tetraethyl orthosilicate (TEOS; 1 ml) in ethanol (10 ml) were added in a dropwise manner into the dispersed solution under continuous mechanical stirring. Finally, FMNPs@SiO_2 was obtained by magnetic separation, and washed with ethanol and deionized water.^[23]

2.2.3 | Preparation of $\text{FMNPs@SiO}_2\text{-Cl}$ (1)

FMNPs@SiO_2 (1 g) was dispersed in 100 ml of dried toluene, and then 3-chloropropyltrimethoxysilane (CPTS; 5 mmol, 1 ml) was added to this mixture. After vigorous stirring for 18 h at 60 °C, the resultant magnetic $\text{FMNPs@SiO}_2\text{-Cl}$ nanoparticles were separated using an external magnet and dried at 60 °C for 3 h.^[24]

2.2.4 | Preparation of 4'-(4-hydroxyphenyl)-2,2':6',2''-terpyridine (TPy)

To a solution of 4-anisaldehyde (0.12 ml, 1 mmol) in ethanol (10 ml) were added 2-acetylpyridine (0.22 ml, 2 mmol) and potassium hydroxide (0.15 g, 2 mmol). After stirring at room temperature, to the mixture was added ammonium hydroxide (2.9 ml, 2.5 mmol) and stirring was continued for 8 h. The resulting precipitate was filtered and recrystallized from ethanol to produce 4'-(4-methoxyphenyl)-2,2':6',2''-terpyridine as white crystals in 85% yield. Then 4'-(4-methoxyphenyl)-2,2':6',2''-terpyridine (0.676 g, 2 mmol) was treated with 30% HBr in acetic acid (4 ml) under reflux condition for 4 h. The mixture was allowed to cool to room temperature. The resultant solution was then basified to pH = 10 by adding aqueous NaOH (20%) dropwise and extracted repeatedly with CH_2Cl_2 . The pH of the alkaline solution was then lowered with HCl (20%). The addition of HCl converted the soluble salt back into water-insoluble TPy as white crystals. The precipitated product was then filtered and collected in 60% yield.^[25]

2.2.5 | Preparation of FMNPs@TPy (2)

To 0.2 g of $\text{FMNPs@SiO}_2\text{-Cl}$ in DMF (3 ml) were added TPy (0.0325 g, 0.1 mmol), K_2CO_3 (0.05 g, 0.4 mmol) and KI (0.05 g, 0.3 mmol). The reaction mixture was stirred at 60 °C for 24 h and then deionized water was added to the mixture. The magnetic nanoparticles were separated with an external magnet. Finally, the precipitate was dried at 50 °C for 2 h to afford FMNPs@TPy in 99% yield.

2.2.6 | Synthesis of FMNPs@TPy-Cu catalyst (3)

FMNPs@TPy-Cu catalyst was prepared in a typical procedure as follows. FMNPs@TPy (0.2325 g) and CuI (0.019 g, 0.1 mmol) were refluxed in ethanol (5 ml) for 24 h. The magnetic nanocatalyst was separated with an external magnet and washed with deionized water to remove the excess Cu^+ and dried at 50 °C for 2 h. The catalyst can be used directly in catalytic reactions.

2.3 | General procedure for synthesis of triazoles

A round-bottom flask was charged with FMNPs@TPy-Cu (0.08 g, containing 0.032 mmol of Cu), potassium carbonate (0.1 g), alkyne (0.5 mmol), sodium azide (0.6 mmol) and alkyl halide (0.5 mmol) in water (2 ml) and ethanol (2 ml). The mixture was stirred at room temperature for 8–24 h, during which the desired 1,4-disubstituted 1,2,3-triazole precipitated out. After completion of the reaction (as monitored by TLC, eluting with *n*-hexane–ethyl acetate, 3:1), the catalyst was separated using an external magnet. The mixture was condensed to evaporate ethanol and diluted with water and EtOAc. The organic layer was separated and the aqueous layer was extracted with EtOAc (3 × 2 ml). The combined organic layers were dried over MgSO_4 and evaporated to afford pure 1,4-disubstituted 1,2,3-triazole in most cases. If necessary, the product was purified by recrystallization from *n*-hexane–EtOAc.

2.4 | General procedure for Cu-catalysed coupling of thiophenols with aryl halides

A mixture of aryl halide (0.5 mmol), thiophenol (0.6 mmol), FMNPs@TPy-Cu catalyst (80 mg containing 0.032 mmol of Cu) and potassium carbonate (0.1 g) was stirred at 110 °C in DMF (1 ml). The progress of the reaction was monitored by TLC (ethyl acetate–hexane). When the reaction was complete, the reaction mixture was cooled to room temperature and the catalyst was separated using an external magnet. The reaction mixture was treated with water (3 ml) and ethyl acetate (10 ml). The organic and aqueous layers were then separated and the aqueous layer was extracted with ethyl acetate (5 ml). The combined organic solutions were washed with water (5 ml) and dried with Na_2SO_4 . The solvent was evaporated under vacuum to afford a colourless liquid of diaryl sulfide. The spectra and physical properties of known products were compared to those reported in the literature.

3 | RESULTS AND DISCUSSION

3.1 | Synthesis and characterization of FMNPs@TPy-Cu Catalyst

In the first phase of the investigation, FMNPs were prepared using a co-precipitation method. In the second stage, the nanoparticles were coated with silica using TEOS. Silica prevents the iron oxide nanoparticles from aggregation or oxidation, but somewhat decreases the saturation magnetization of FMNPs. To stabilize the ligand on the magnetic nanoparticles through a covalent bond linkage, CPTS was used to modify the surface of the nanoparticles.

The ligand TPy was readily prepared and reacted with $\text{FMNPs@SiO}_2\text{-Cl}$ (1) in the presence of K_2CO_3 to afford FMNP@TPy (2). The ligand has nitrogen atoms in the rings

servicing as multiple interaction sites and forms stable coordinated complex with Cu^+ (3) as indicated in Scheme 3.

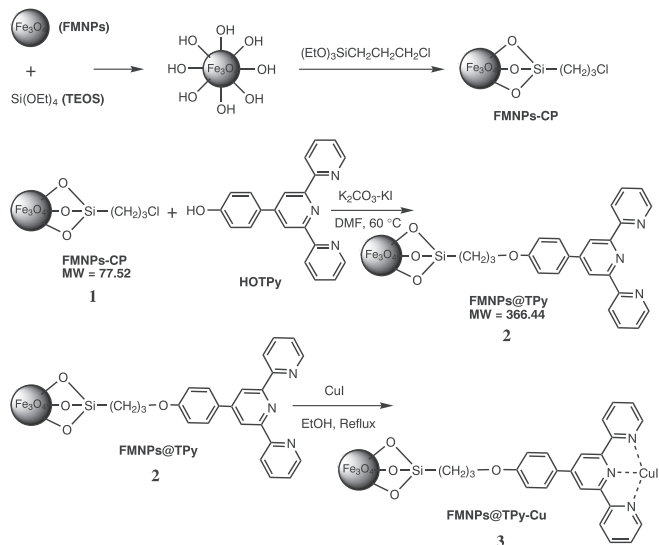
After the successful preparation of immobilized ligand on the surface of shell (FMNPs@TPy), the optimal loading amount of CuI was investigated. It is found that a 1:1 mole ratio of ligand to copper iodide is the best choice. The obtained catalyst was fully characterized using FT-IR spectroscopy, XRD, SEM, TEM, EDX and VSM.^[26]

3.1.1 | FT-IR spectroscopy

The successful synthesis of the Fe_3O_4 nanoparticles was confirmed from the FT-IR spectra (Figure 1). The signal observed at 579 cm^{-1} is attributed to the Fe—O bond vibration. The broad peaks at around $3200\text{--}3500\text{ cm}^{-1}$ are ascribed to the stretching vibrations of hydrogen-bonded surface water molecules in atmosphere and hydroxyl groups, which are located on the surface of the iron oxide nanoparticles. These broad peaks may also indicate the presence of some amount of ferric hydroxide in Fe_3O_4 (Figure 1a). In the case of FMNPs@ SiO_2 (Figure 1b), the sharp band at 1087 cm^{-1} corresponds to Si—O—Si antisymmetric stretching. The peak at 807 cm^{-1} is due to the symmetric stretching vibration of Si—O—Si. These results indicate the coating of silica on the surface of FMNPs. The band observed at 1661 cm^{-1} could be attributed to the C=N (pyridine ring) stretching frequency (Figure 1c). The C=N band of the FMNPs@TPy-Cu complex is shifted to a lower frequency (1594 cm^{-1}) compared to that of FMNPs@TPy (Figure 1d). The lowering in frequency of the C=N peak is indicative of the formation of a metal–ligand bond. Also the peak at 1228 cm^{-1} is assigned to the C—O stretching vibration of phenolic group.

3.1.2 | X-ray diffraction

In this work, the crystalline structures of FMNPs@ SiO_2 (Figure 2a), TPy-Cu (Figure 2b) and FMNPs@TPy-Cu



SCHEME 3 Preparation of FMNPs@TPy-Cu (3)

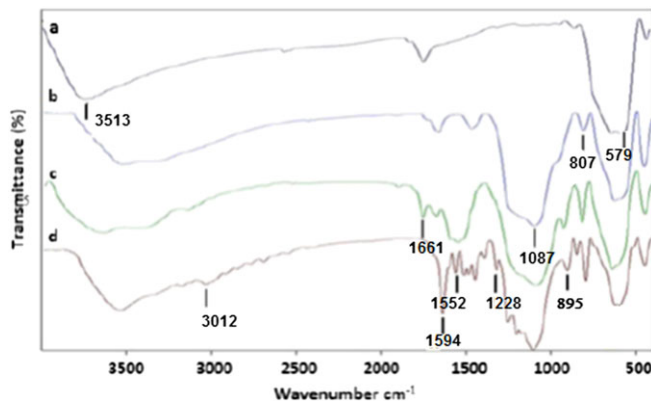


FIGURE 1 FT-IR spectra: (a) FMNPs; (b) FMNPs@ SiO_2 ; (c) FMNPs@TPy; (d) FMNPs@TPy-Cu

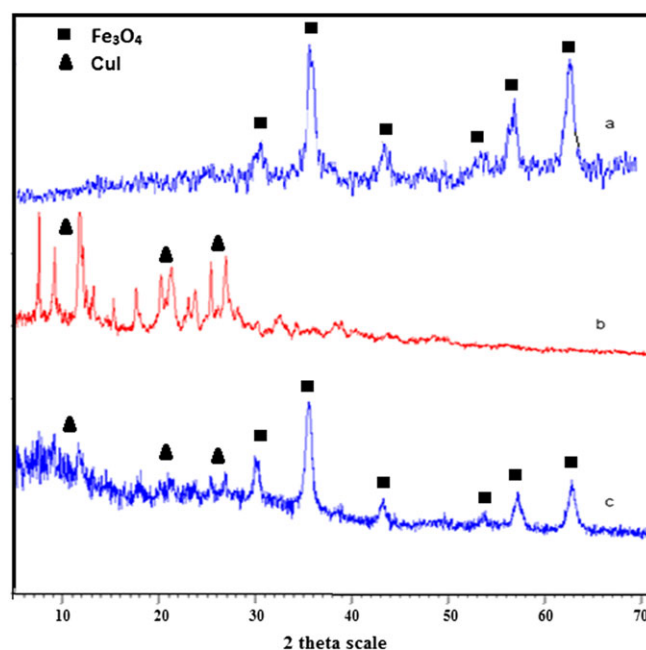


FIGURE 2 XRD patterns: (a) FMNPs@ SiO_2 ; (b) TPy-Cu; (c) FMNPs@TPy-Cu

(Figure 2c) were analysed using XRD. The XRD pattern of Fe_3O_4 exhibits peaks at $2\theta = 30.2^\circ, 35.6^\circ, 43.3^\circ, 53.6^\circ, 57.3^\circ$ and 62.8° corresponding to diffraction lines (220), (311), (400), (422), (511) and (440), respectively, which conform well to the reported values.^[27] The XRD patterns (Figure 2) show that no change occurs in the crystalline structure of Fe_3O_4 after silica modification with TEOS and CPTS. Also, the XRD pattern shows the sharp peaks of copper complex with terpyridine (Figure 2b). In Figure 2(c), the appearance of peaks at lower than 30° confirms the presence of copper in the catalyst. The data relating to XRD pattern of the catalyst are summarized in Table 1. The signal appearing at $2\theta = 25.5^\circ$ corresponds to the (111) plane of copper.^[28]

The average crystallite size (D) for the designed FMNPs@TPy-Cu catalyst was calculated using the Debye–Scherrer equation: $D = K\lambda/(\beta \cos \theta)$, with λ being the X-ray wavelength (0.154 nm), K the Scherrer constant (0.9), β the

TABLE 1 Analysis of XRD patterns relating to FMNPs@TPy-Cu

Position, 2θ ($^\circ$)	Height (cts)
11.9	113
20.3	52
25.5	54
27.0	73
30.2	148
35.7	619
43.2	91
53.7	44
57.3	127
62.9	191

peak width of half maximum and θ the Bragg diffraction angle.^[29] The crystallite size of the catalyst (D), obtained at a peak of say $2\theta = 35.731^\circ$ ($\theta = 17.8655^\circ$, $\cos \theta = 0.554$), is found to be about 22 nm.

3.1.3 | Thermogravimetric analysis

The thermal behaviour of FMNPs@SiO₂-Cl and the catalyst is shown in Figure 3. The amount of organic moieties attached to FMNPs was measured using TGA. The TGA plots of FMNPs@SiO₂ and FMNPs@TPy-Cu show that thermal decomposition occurs in two steps. The first step weight loss up to 200–220 °C corresponds to removal of physically and chemically adsorbed water, whereas, at temperature higher than 220 °C, the main weight loss (second step) is due to removal of organic moieties from the surface. Also, the TGA results indicate that the catalyst has very high thermal stability (about 600 °C).

The TGA results are summarized in Table 2. The observed total weight loss based on theoretical calculation corresponds to 93.4% in conversion for the stage of FMNPs@SiO₂-Cl to FMNPs@TPy-Cu.

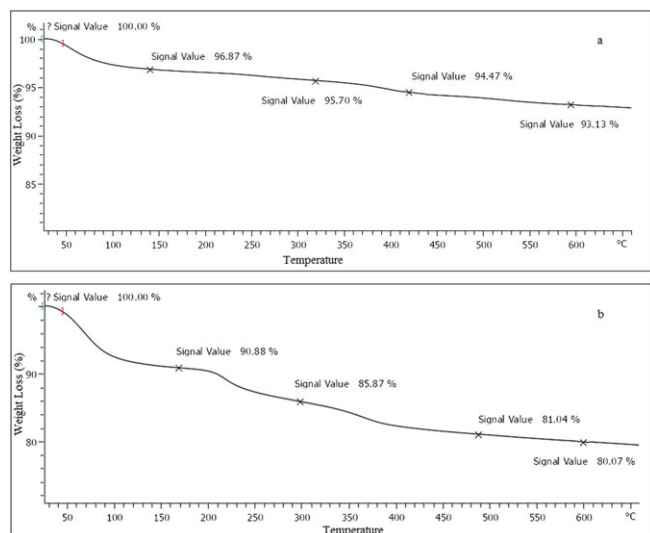
FIGURE 3 TGA curves: (a) FMNPs@SiO₂-Cl; (b) FMNPs@TPy-Cu

TABLE 2 TGA results

Sample	Reduced weight at 600 °C (wt%) ^a	Organic weight (%) ^b	Yield (%)
FMNPs@SiO ₂ -Cl	6.87	—	—
FMNPs@TPy-Cu	19.93	13.98	93.4

^aExperimental ligand part in the catalyst = 19.93–6.87 = 13.06.

^bTheoretical ligand part in the catalyst = 13.98.

3.1.4 | EDX spectroscopy

The EDX spectrum of the obtained nanocatalyst indicates the presence of iron, oxygen, nitrogen, carbon, silicon and copper elements in its structure (Figure 4). The signal of Fe is attributed to Fe₃O₄, Si and O correspond to SiO₂, C and N are related to TPy and Cu is assigned to CuI. The spectrum confirms that FMNPs are coated with silica, modified with TPy and complexed with CuI.

3.1.5 | Transmission electron microscopy

TEM images of FMNPs@TPy-Cu catalyst are presented in Figure 5. The dark coloured regions or black spots in the image of the core-shell correspond to the nano-Fe₃O₄, while the colourless parts represent silica. Figure 5(c) shows that two small spots might indicate the presence of copper

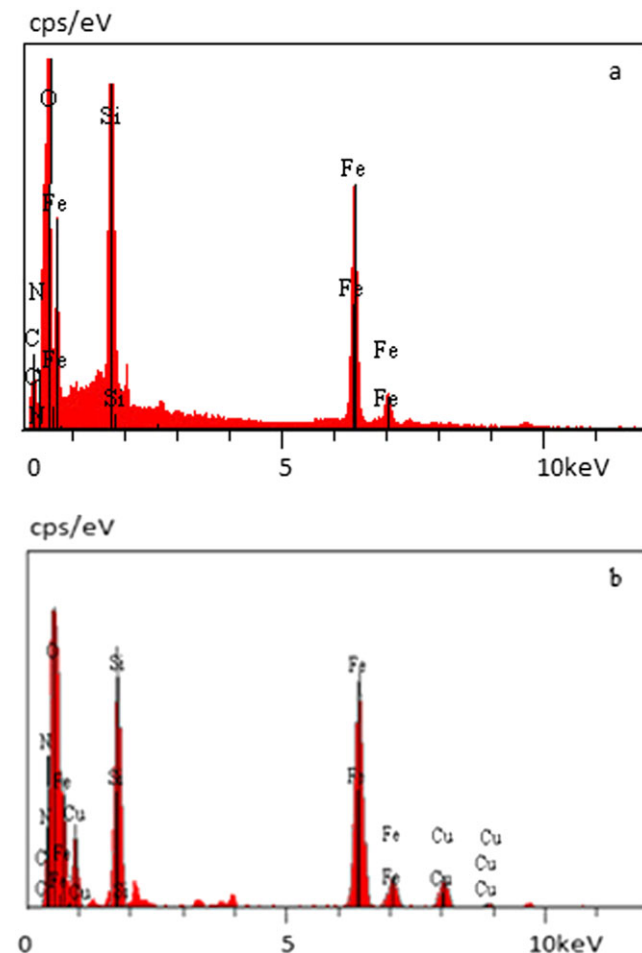


FIGURE 4 EDX patterns: (a) FMNPs@TPy; (b) FMNPs@TPy-Cu

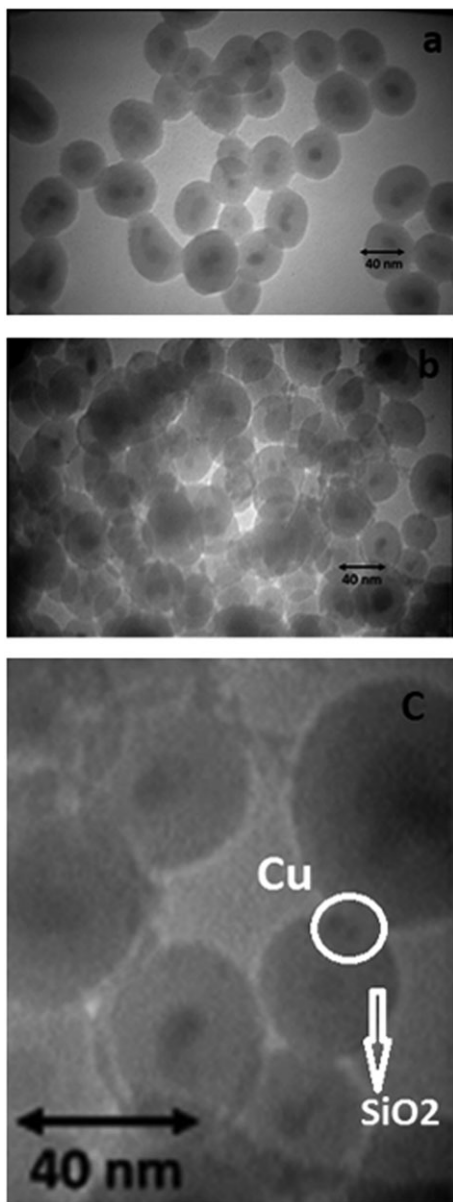


FIGURE 5 TEM images: (a) FMNPs@SiO₂-Cl; (b, c) FMNPs@TPy-Cu

nanoparticles on the surface of the silica shell in the structure of the catalyst.

3.1.6 | Scanning electron microscopy

The SEM image (Figure 6) shows that FMNPs@TPy-Cu has a mean diameter of about 40 nm and a nearly spherical shape. The nanoparticles are well dispersed and uniform in shape and size, which is consistent with XRD results and TEM images.

3.1.7 | Magnetic properties

The magnetic properties of FMNPs@SiO₂-Cl and FMNPs@TPy-Cu were characterized using VSM. The saturation magnetization (M_s) of FMNPs is 62.8 emu g⁻¹. This M_s is affected by various factors including size, shape,

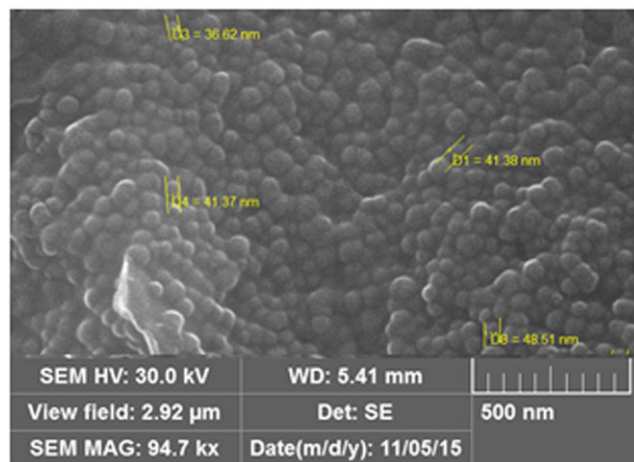


FIGURE 6 SEM image of FMNPs@TPy-Cu

composition and shell-core structure. The magnetization curves for FMNPs@SiO₂-Cl and the obtained nanocatalyst are depicted in Figure 7. The saturation magnetizations are found to be 25.5 and 19.7 emu g⁻¹ for FMNPs@SiO₂-Cl and FMNPs@TPy-Cu, respectively, which are much lower than that of bare FMNPs. This can be attributed to the coating of silica on the magnetic nanoparticles.^[30]

3.2 | Catalytic studies of Fe₃O₄@TPy-Cu nanocatalyst

3.2.1 | Synthesis of triazoles from sodium azide and terminal acetylenes

The catalytic activity of the Fe₃O₄@TPy-Cu nanocatalyst was examined in an efficient and convenient preparation of 1,4-disubstituted 1,2,3-triazoles using a simple one-pot three-component reaction of primary halides, sodium azide and terminal acetylenes at room temperature (Scheme 1). The catalyst was easily recovered using an external magnet and was reused in at least five successive runs without an appreciable loss of activity (Figure 8).

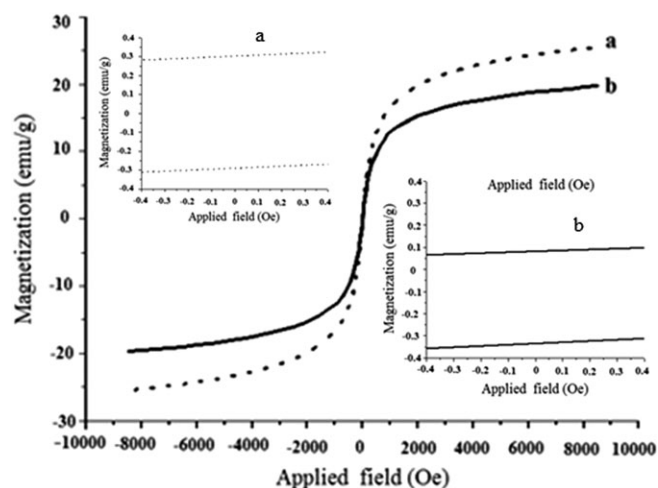


FIGURE 7 VSM magnetization curves: (a) FMNPs@SiO₂; (b) FMNPs@TPy-Cu

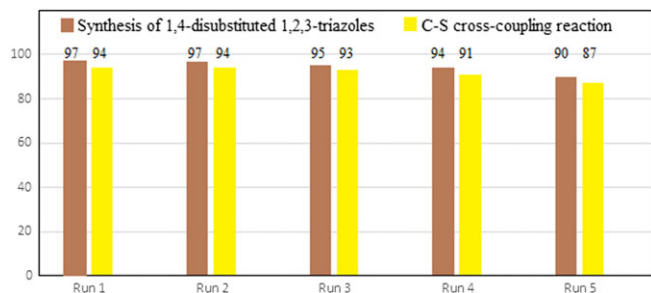


FIGURE 8 Catalytic activity and reusability of magnetically separable Cu-based catalyst

We chose benzyl bromide and phenyl acetylene as model substrates, and their reaction was investigated with sodium azide in the presence of FMNPs@TPy-Cu under various aerobic conditions (Table 3). The reaction rates are markedly dependent on the amount of catalyst, base and solvent. Therefore, the application of FMNPs@TPy-Cu was examined with the optimization of the reaction conditions. It is evident from Table 3 (entry 12) that the best result is obtained when K_2CO_3 is used as a base, 0.032 mmol of Cu loaded and a mixture of water and ethanol (1:1) applied as a solvent. The presence of ethanol as a co-solvent leads to an improved solubility of the substrates. Water, dimethylsulfoxide (DMSO), DMF, tetrahydrofuran (THF), ethanol and water with co-solvents such as DMSO, DMF and ethanol were evaluated as a solvent and bases such as NEt_3 , K_2CO_3 , Na_2CO_3 , $NaHCO_3$, NaOH and KOH were examined in this reaction (Table 3).

TABLE 3 Optimization of reaction conditions for synthesis of 1,4-disubstituted 1,2,3-triazoles^a

Entry	FMNPs@TD-Cu (g)	Base	Solvent	Yield (%) ^b
1	—	K_2CO_3	$H_2O-EtOH$ (1:1)	Trace
2	0.04	K_2CO_3	H_2O	35
3	0.06	K_2CO_3	H_2O	67
4	0.08	K_2CO_3	H_2O	78
5	0.1	K_2CO_3	H_2O	78
6	0.06	K_2CO_3	DMSO	74
7	0.08	K_2CO_3	DMF	85
8	0.08	K_2CO_3	THF	80
9	0.08	K_2CO_3	EtOH	83
10	0.08	K_2CO_3	$H_2O-DMSO$ (1:1)	88
11	0.08	K_2CO_3	H_2O-DMF (1:1)	92
12	0.08	K_2CO_3	$H_2O-EtOH$ (1:1)	97
13	0.08	$NaHCO_3$	$H_2O-EtOH$ (1:1)	64
14	0.08	NaOH	$H_2O-EtOH$ (1:1)	78
15	0.08	KOH	$H_2O-EtOH$ (1:1)	80
16	0.08	NEt_3	$H_2O-EtOH$ (1:1)	79

^aReaction conditions: phenylacetylene (1.2 mmol), NaN_3 (1 mmol), benzyl bromide (1 mmol), catalyst (80 mg), solvent (4 ml), 25 °C.

^bIsolated yield.

To evaluate the generality of this reaction, we investigated the reactions using *n*-butylacetylene and hydroxymethylacetylene instead of phenylacetylene. Also, the reactions of phenylacetylene, sodium azide and ring-substituted benzyl bromides, bromoacetophenones and allyl bromide were carried out under the optimized reaction conditions. The results are collected in Table 4. The results show that the nature of the substituent does not have a considerable effect on the yield and the time of the reaction. However, the reactions with alkylacetylenes compared with phenylacetylene proceed in longer reaction times and with lower yields of products (Table 4, entries 3 and 4). Presumably in the case of phenylacetylene, the aromatic ring promotes the reaction.

In addition, it must be noted that negligible Cu leaching is found in the reaction in a similar way as already reported in the literature.^[31] To test for leaching, the catalyst in the reaction of benzyl bromide, phenylacetylene and sodium azide was removed after 3 h and the reaction was permitted to continue under the same reaction conditions in the absence of the catalyst. We observed that the reaction without the catalyst was not completed.

3.2.2 | C–S cross-coupling reaction

In recent years, a series of synthetic protocols have been reported for the formation of C–S bonds and especially the preparation of arylalkyl and diaryl sulfides through cross-coupling reactions using copper nanoparticles as catalyst.

TABLE 4 One-pot synthesis of 1,4-disubstituted 1,2,3-triazoles^a

Entry	R ¹	X	R ²	Time (h)	Yield (%) ^b
1	C ₆ H ₅	Br	C ₆ H ₅ CH ₂	8	97
2	C ₆ H ₅	Cl	C ₆ H ₅ CH ₂	8	96
3	CH ₂ OH	Br	C ₆ H ₅ CH ₂	13	85
4	CH ₂ OH	Cl	C ₆ H ₅ CH ₂	13	83
5	<i>n</i> -C ₄ H ₉	Br	C ₆ H ₅ CH ₂	16	89
6	C ₆ H ₅	Br	O ₂ NC ₆ H ₄ CH ₂	8	93
7	C ₆ H ₅	Br	MeC ₆ H ₄ CH ₂	9	90
8	C ₆ H ₅	Br	PhC ₆ H ₄ CH ₂	9	91
9	C ₆ H ₅	Cl	MeOC ₆ H ₄ CH ₂	10	90
10	C ₆ H ₅	Br	C ₆ H ₅ COCH ₂	9	87
11	C ₆ H ₅	Br	4-BrC ₆ H ₄ COCH ₂	10	85
12	C ₆ H ₅	Br	CH ₂ =CHCH ₂	8	94

^aThree-component reaction conditions: alkyne (1.2 mmol), NaN₃ (1 mmol), alkyl halide (1 mmol), catalyst (80 mg), H₂O–EtOH (4 ml), 25 °C.

^bIsolated yield.

The magnetic nanocatalysts of copper are efficient catalysts for C–S coupling reactions. In this work, copper(I) supported on functionalized FMNPs was used as an efficient and magnetically recoverable catalyst for C–S cross-coupling reactions of aryl halides with thiols (Scheme 2). It is notable that after completion of the reaction, the catalyst was separated from the mixture using an external magnet, washed with deionized water and ethanol, and then dried. It can be reused up to five times without significant decrease in efficiency (Figure 8).

Initially, we examined the coupling of iodobenzene with thiophenol as a model reaction in the presence of various amounts of catalysts, and with a variety of bases and solvents. It is found that using iodobenzene (1 mmol), thiophenol (1 mmol) and K₂CO₃ (0.1 g) in the presence of nanocatalyst (0.08 g, 0.032 mmol Cu) in DMF at 110 °C affords the desired product in 94% yield (Table 5). It is seen that DMF/K₂CO₃ system has a good compatibility in the product yield.

To define the scope of the FMNPs@TPy-Cu-catalysed coupling reaction, we investigated the reactivity of thiophenol, *p*-nitrothiophenol and *p*-methylthiophenol with various substituted aryl halides under optimized conditions. In general, all reactions are very clean and this protocol gives the corresponding thioethers in good to excellent yields (Table 6, entries 1–16). The reactions with aryl bromides afford slightly lower yields and require longer reaction times (Table 6, entries 7–9). The small decrease in the yield of *o*-product (Table 6, entries 3 and 5) can be ascribed to steric hindrance at the substrates. It must be noted that when 2-iodothiophene is used, the desired product is obtained in 90% yield and no poisoning of the catalyst is observed. Aryl chlorides are not reactive under these reaction conditions

TABLE 5 Optimization of reaction conditions for synthesis of diphenyl sulfide

Entry	FMNPs@TPy-Cu (g)	Base	Solvent	Yield (%) ^b
1	0.04	K ₂ CO ₃	DMF	35
2	0.06	K ₂ CO ₃	DMF	67
3	0.08	K₂CO₃	DMF	94
4	0.1	K ₂ CO ₃	DMF	94
5	0.08	Na ₂ CO ₃	DMF	74
6	0.08	KOH	DMF	82
7	0.08	NaOH	DMF	80
8	0.08	Et ₃ N	DMF	53
9	0.08	NaOBu ^t	DMF	86
10	0.08	K ₂ CO ₃	Toluene	69
11	0.08	K ₂ CO ₃	DMSO	83
12	0.08	K ₂ CO ₃	THF	53
13	0.08	K ₂ CO ₃	EtOH	50

^aReaction conditions: iodobenzene (1 mmol), thiophenol (1.2 mmol), base (3.0 mmol), solvent (3 ml), FMNPs@TPy-Cu (80 mg), 6 h.

^bIsolated yield.

(Table 6, entry 17). Unfortunately, an attempt to couple an aliphatic thiol (Table 6, entry 18) with aryl halides failed.

3.2.3 | Reusability of catalyst

The reusability of the catalyst was studied during the preparation of 1,4-disubstituted 1,2,3-triazoles and thioethers. After completion of the reaction, the catalyst was easily removed

TABLE 6 C–S cross-coupling reactions of aryl halides and thiols^a

$\text{ArS-H} + \text{Ar}'\text{-X} \xrightarrow[\text{K}_2\text{CO}_3, \text{DMF}, 110\text{ }^\circ\text{C}]{\text{FMNPs@Cu-TPy}} \text{ArS-Ar}'$					
Entry	Ar	X	Ar'	Time (h)	Yield (%) ^b
1	C ₆ H ₅	I	C ₆ H ₅	5	94
2	C ₆ H ₅	I	4-MeC ₆ H ₄	5	92
3	C ₆ H ₅	I	2-MeC ₆ H ₄	6	90
4	C ₆ H ₅	I	4-MeOC ₆ H ₄	5	91
5	C ₆ H ₅	I	2-MeOC ₆ H ₄	7	89
6	C ₆ H ₅	I	C ₄ H ₃ S	5	90
7	C ₆ H ₅	Br	C ₆ H ₅	10	87
8	C ₆ H ₅	Br	4-MeC ₆ H ₄	10	86
9	C ₆ H ₅	Br	4-O ₂ NC ₆ H ₄	8	90
10	C ₆ H ₅	Br	C ₆ H ₅ CH ₂	5	95
11	C ₆ H ₅	Br	4-BrC ₆ H ₄	5	90
12	C ₆ H ₅	Br	4-MeC ₆ H ₄ CH ₂	5	92
13	4-MeC ₆ H ₄	I	C ₆ H ₅	5	95
14	4-MeC ₆ H ₄	I	4-MeC ₆ H ₄	5	91
15	4-MeC ₆ H ₄	I	4-MeOC ₆ H ₄	6	89
16	4-NO ₂ C ₆ H ₄	I	C ₆ H ₅	7	85
17	C ₆ H ₅	Cl	C ₆ H ₅	24	Trace
18	<i>n</i> -C ₄ H ₉	I	C ₆ H ₅	24	Trace

^aReaction conditions: aryl halide (0.5 mmol), ArSH (0.5 mmol), DMF (1 ml), K₂CO₃ (0.1 g), catalyst (80 mg), 110 °C.

^bIsolated yield.

using an external magnet. It was simply recovered by successively washing with organic solvent (ethanol) and vacuum drying. The catalyst was tested for five consecutive runs and, through each run, no fresh catalyst was added. For example, the reaction of phenylacetylene, benzyl bromide and sodium azide affords the corresponding 1,4-disubstituted 1,2,3-triazole five times in sequence (Figure 8). As the results in Figure 8 show, the catalyst can be used several times without any appreciable loss of its initial catalytic activity. To determine the catalyst leaching into solution, atomic absorption spectroscopy (AAS) was used to measure the amount of copper before and after five successive runs using FMNPs@TPy-Cu. The amount of copper attached on fresh catalyst is 2.16% based on the AAS results, while the amount of copper decreases to 2.15% after five sequential reuses. Hence, the amount of copper leached from the catalyst is 0.01% after five runs, which is negligible, and this is due to strong interaction between copper and catalyst.

4 | CONCLUSIONS

A novel and efficient catalyst of terpyridine/CuI immobilized on ferromagnetic nanoparticles through a surface modification (FMNPs@TPy-Cu) has been prepared and characterized for the regioselective synthesis of 1,4-disubstituted 1,2,3-triazoles

and the synthesis of thioethers from C–S cross-coupling reactions of thiols and aryl halides.

This highly active heterogeneous nanocatalyst has a very high surface area, and its thermal and chemical stabilities were confirmed using various characterization techniques. This recoverable and reusable catalyst is benign, of low cost and can be handled easily.

ACKNOWLEDGEMENT

The authors thank the Razi University Council for support of this work.

REFERENCES

- [1] a) M. Jones, C. Cooper, M. F. Mahon, P. R. Raithby, D. Apperley, J. Wolowska, D. Collison, *J. Mol. Catal. A: Chem.* **2010**, 325, 8; b) J. Safaei-Ghomi, S. Rohani, A. Ziarati, *J. NanoStructures* **2012**, 2, 79; c) B. N. Lin, S. H. Huang, W. Y. Wu, C. Y. Mou, F. Y. Tsai, *Molecules* **2010**, 15, 9157; d) J. Liu, L. Chen, H. Cui, J. Zhang, L. Zhang, C. Y. Su, *Chem. Soc. Rev.* **2014**, 43, 6011.
- [2] Z. M. Michalska, *Met. Rev.* **1974**, 18, 65.
- [3] a) K. G. Thomas, P. V. Kamat, *Acc. Chem. Res.* **2003**, 36, 888; b) M. Qhobosheane, S. Santra, P. Zhang, W. Tan, *Analyst* **2001**, 126, 1274.
- [4] S. Shylesh, V. Schunemann, W. R. Thiel, *Angew. Chem. Int. Ed.* **2010**, 49, 3428.
- [5] a) M. J. Jin, D. H. Lee, *Angew. Chem. Int. Ed.* **2010**, 49, 1119; b) Z. Yinghuai, S. C. Peng, A. Emi, S. Zhenshun, R. A. Kemp, *Adv. Synth. Catal.* **2007**, 349, 1917; c) X. Jin, K. Zhang, J. Sun, J. Wang, Z. Dong, R. Li, *Catal. Commun.* **2012**, 26, 199.

- [6] a) C. W. Tornøe, C. Christensen, M. Meldal, *J. Org. Chem.* **2002**, *67*, 3057; b) V. V. Rostovtsev, L. G. Green, V. V. Fokin, K. B. Sharpless, *Angew. Chem. Int. Ed.* **2002**, *41*, 2596; c) R. Huisgen, *Angew. Chem.* **1963**, *75*, 604.
- [7] a) H. Nandivada, X. Jiang, J. Lahann, *Adv. Mater.* **2007**, *19*, 2197; b) Y. L. Angella, K. Burgess, *Chem. Soc. Rev.* **2007**, *36*, 1674; c) J. F. Lutz, *Angew. Chem. Int. Ed.* **2007**, *46*, 1018.
- [8] a) S. Haider, M. S. Alam, H. Hamid, *Inflamm. Cell Signal.* **2014**, *1*; b) S. G. Agalave, S. R. Maujan, V. S. Pore, *Chem. – Asian J.* **2011**, *6*, 2696.
- [9] a) L. Zhang, X. Chen, P. Xue, H. H. Y. Sun, I. D. Williams, K. B. Sharpless, V. V. Fokin, *J. Am. Chem. Soc.* **2005**, *127*, 15998; b) S. Díez-González, A. Correa, L. Cavallo, S. P. Nolan, *Chem. – Eur. J.* **2006**, *12*, 7558; c) S. Díez-González, S. P. Nolan, *Synlett* **2007**, 2158.
- [10] a) H. A. Stefani, S. N. S. Vasconcelos, F. B. Souza, F. Manarin, J. Zukerman-Schpector, *Tetrahedron Lett.* **2013**, *54*, 5821; b) Y. B. Zhao, Z. Y. Yan, Y. M. Liang, *Tetrahedron Lett.* **2006**, *47*, 1545; c) J. Vantikommu, S. Palle, P. S. Reddy, V. Ramanatham, M. Khagga, V. R. Pallapothula, *J. Med. Chem.* **2010**, *45*, 5044; d) N. W. Smith, B. P. PolenZ, S. B. Johnson, S. V. Dzyuba, *Tetrahedron Lett.* **2010**, *51*, 550.
- [11] a) B. Sreedhar, P. S. Reddy, V. R. Krishna, *Tetrahedron Lett.* **2007**, *48*, 5831; b) A. Pathigoolla, R. P. Pola, K. M. Sureshan, *Appl. Catal. A* **2013**, *453*, 151; c) V. Ganesh, V. S. Sudhir, T. Kundu, S. Chandrasekaran, *Chem. – Asian J.* **2011**, *6*, 2670.
- [12] a) F. Himo, T. Lovell, R. Hilgraf, V. V. Rostovtsev, L. Noodleman, K. B. Sharpless, V. V. Fokin, *J. Am. Chem. Soc.* **2005**, *127*, 210; b) N. Gommermann, A. Gehrig, P. Knochel, L. Maximilians, *Synlett* **2005**, 2796; c) G. Cravotto, V. V. Fokin, D. Garella, A. Binello, L. Boffa, A. Barge, *J. Comb. Chem.* **2010**, *12*, 13; d) Q. Wang, S. Chittaboina, H. N. Barnhill, *Lett. Org. Chem.* **2005**, *2*, 293; e) H. A. Orgueira, D. Fokas, Y. Isome, P. C. M. Chan, C. M. Baldino, *Tetrahedron Lett.* **2005**, *46*, 2911.
- [13] a) M. L. Kantam, V. S. Jaya, B. Sreedhar, M. M. Rao, B. M. Choudary, *J. Mol. Catal. A* **2006**, *256*, 273; b) S. Chassaing, A. S. S. Sido, A. Alix, M. Kumarraja, P. Pale, J. Sommer, *Chem. – Eur. J.* **2008**, *14*, 6713; c) F. Nador, M. A. Volpe, F. Alonso, A. Feldhoff, A. Kirschning, G. Radivoy, *Appl. Catal. A* **2013**, *455*, 39; d) K. Martina, S. E. S. Leonhardt, B. Ondruschka, M. Curini, A. Binello, G. Cravotto, *J. Mol. Catal. A* **2011**, *334*, 60; e) Y. Monguchi, K. Nozaki, T. Maejima, Y. Shimoda, Y. Sawama, Y. Kitamura, Y. Kitade, H. Sajiki, *Green Chem.* **2013**, *15*, 490.
- [14] a) D. J. Procter, *J. Chem. Soc. Perkin Trans. I* **2001**, 335; b) T. Kondo, T. Mitsudo, *Chem. Rev.* **2000**, *100*, 3205.
- [15] a) S. F. Nielsen, E. Nielsen, G. M. Olsen, T. Liljefors, D. Peters, *J. Med. Chem.* **2000**, *43*, 2217; b) Y. Wang, S. Chackalamannil, Z. Hu, J. W. Clader, W. Greenlee, W. Billard, H. Binch, G. Crosby, V. Ruperto, R. A. Duffy, R. McQuade, J. E. Lachowicz, *Bioorg. Med. Chem. Lett.* **2000**, *10*, 2247.
- [16] M. Kosugi, T. Ogata, M. Terada, H. Sano, T. Migita, *Bull. Chem. Soc. Jpn.* **1985**, *58*, 3657.
- [17] a) T. Itoh, T. Mase, *Org. Lett.* **2004**, *6*, 4587; b) M. A. Fernández-Rodríguez, Q. Shen, J. F. Hartwig, *J. Am. Chem. Soc.* **2006**, *128*, 2180; c) M. A. Fernández-Rodríguez, Q. Shen, J. F. Hartwig, *Chem. – Eur. J.* **2006**, *12*, 7782.
- [18] a) S. Jammi, P. Barua, L. Rout, P. Saha, T. Punniyamurthy, *Tetrahedron Lett.* **2008**, *49*, 1484; b) A. Saxena, A. Kumar, S. Mozumdar, *Appl. Catal. A* **2007**, *317*, 210.
- [19] Y. C. Wong, T. T. Jayanth, C. H. Cheng, *Org. Lett.* **2006**, *8*, 5613.
- [20] a) M. Carril, R. SanMartin, E. Dominguez, I. Tellitu, *Chem. – Eur. J.* **2007**, *13*, 5100; b) A. K. Verma, J. Singh, R. Chaudhary, *Tetrahedron Lett.* **2007**, *48*, 7199; c) Y. S. Feng, Y. Y. Li, L. Tang, W. Wu, H. J. Xu, *Tetrahedron Lett.* **2010**, *51*, 2489; d) Y. Liu, H. Wang, X. Cao, Z. Fang, J. P. Wan, *Synthesis* **2013**, *45*, 2977; e) L. Rout, K. S. Tamal, T. Punniyamurthy, *Angew. Chem. Int. Ed.* **2007**, *46*, 5583.
- [21] a) A. Alizadeh, M. M. Khodaei, D. Kordestani, A. H. Fallah, M. Beygzadeh, *Micropor. Mesopor. Mater.* **2012**, *159*, 9; b) A. Alizadeh, M. M. Khodaei, M. Beygzadeh, D. Kordestani, M. Feyzi, *Bull. Korean Chem. Soc.* **2012**, *33*, 2546; c) A. Alizadeh, M. M. Khodaei, C. Karami, M. S. Workentin, M. Shamsipur, M. Sadeghi, *Nanotechnology* **2010**, *21*, 315503.
- [22] D. Yang, J. Hu, S. Fu, *J. Phys. Chem. C* **2009**, *113*, 7646.
- [23] W. Stober, A. Fink, E. Bohn, *J. Colloid Interface Sci.* **1968**, *26*, 62.
- [24] a) F. Sulek, M. Drogenik, M. Habulin, Z. Knez, *J. Magn. Magn. Mater.* **2010**, *322*, 179; b) P. Jal, S. Patel, B. Mishra, *Talanta* **2004**, *62*, 1005.
- [25] a) V. W. Spahni, G. Calzaferri, *Helv. Chim. Acta* **1984**, *67*, 450; b) I. Eryazici, N. Moorefield, R. Newkome, *Chem. Rev.* **2008**, *108*, 1834.
- [26] M. Gao, W. Li, J. Dong, Z. Zhang, B. Yang, *World J. Condens. Matter Phys.* **2011**, *1*, 49.
- [27] M. Tajbakhsh, M. Farhang, R. Hosseinzadeh, Y. Sarrafi, *RSC Adv.* **2014**, *4*, 23116.
- [28] M. N. Soltani Rad, S. Behrouz, M. M. Doroodmand, A. Movahediyani, *Tetrahedron* **2012**, *68*, 7812.
- [29] a) K. Kacprzak, *Synlett* **2005**, 6, 943; b) A. Pathigoolla, R. P. Pola, K. M. Sureshan, *Appl. Catal. A* **2013**, *453*, 151; c) J. Albadi, M. Keshavarz, F. Shirini, M. Vafaei-nezhad, *Catal. Commun.* **2012**, *27*, 17.
- [30] R. K. Sharma, M. Yadav, Y. Monga, R. Gaur, A. Adholeya, R. Zboril, R. S. Varma, M. B. Gawande, *ACS Sustain. Chem. Eng.* **2016**, *4*, 1123.
- [31] L. Yin, J. Liebscher, *Chem. Rev.* **2007**, *107*, 133.

SUPPORTING INFORMATION

Additional Supporting Information may be found online in the supporting information tab for this article.

How to cite this article: Khodaei MM, Bahrami K, Meibodi FS. Ferromagnetic nanoparticle-supported copper complex: A highly efficient and reusable catalyst for three-component syntheses of 1,4-disubstituted 1,2,3-triazoles and C–S coupling of aryl halides. *Appl Organometal Chem.* 2017;e3714. <https://doi.org/10.1002/aoc.3714>